Study of monolithic CMOS pixel sensors in the Belle II experiment upgrade

October 26, 2023

Contents

Introduction **4**

1 Belle II and SuperKEKB (SKB) accelerator **6**

1.1 Physics program of the B-factories 6

1.1.1 Open questions in SM 7

1.1.2 Peculiarity of asymmetric B factories 7

1.2 SuperKEKB accelerator 9

1.2.1 The facility 9

1.2.2 "Nano-beam" scheme 10

1.3 Belle II detector 11

1.3.1 Vertex Detectors (VXD) 11

1.3.2 Central Drift Chamber (CDC) 12

1.3.3 Particle identification system (TOP e ARICH) 13

1.3.4 Electromagnetic calorimeter (ECL) 15

1.3.5 K_L muon detector (KLM) 15

1.3.6 Trigger system 15

1.4 Current state of data taking 16

2 CMOS MAPS sensors **18**

2.1 Semiconductor detectors 18

2.2 Hybrid and monolithic pixel sensors 18

2.3 CMOS Monolithic Active Pixel Sensors technology 18

2.4 History of Monopix developments 18

3 Conclusions **19**

List of Figures **20**

List of Tables **21**

Introduction

Belle II is a particle physics experiment located at KEK laboratory in Tsukuba (Japan), 100 km away from Tokyo. The detector is a general-purpose spectrometer and it is placed along the SuperKEKB accelerator, a second generation flavor-factory which operates at the luminosity frontier, holding the world record of istantaneous luminosity with $L_{ist} = 4.7 \times 10^{34}\ cm^{-2}s^{-1}$.

SuperKEKB is the upgrade of the preceding facility KEKB (operational from 1998 to 2016) and it consists in a 3 km-circumference asymmetric accelerator which collides electrons and positrons beams (with energy of 7 GeV and 4 GeV, respectively) at a center-of-mass energy near the $\Upsilon(4S)$ resonance ($\sqrt{s} = 10.58$ GeV). It started its data taking in March 2019.

In the first years of the next decade, the collider aims to collect an unrivaled dataset of 50 ab^{-1} (x50 Belle dataset, x100 BaBar dataset) and to reach a new peak of istantaneous luminosity, in order to study the charge-parity violation in B mesons system with more precision and to search for new hints of pyhsics beyond the Standard Model.

To achieve these challenging targets, it would be necessary a significant upgrade of the accelerator and its main components (in particular nearby the Interaction Region) and also of the detector. As a matter of fact, to the increase in luminosity corresponds not only large data collected and greater possibility to study rare processes, but also higher doses of radiation and greater level of backgrounds which could undermine the integrity and the operation of the Belle II detector. In particular the subdetectors which are nearer to the beam pipe are those more exposed to severe conditions, like the vertex detector (VXD), composed by the inner pixel detector (PXD, made by layers of pixel) and the outermost silicon vertex detector (SVD, made by layers of strips). They deal with the reconstruction of charged particle tracks and of decay vertices with high performance. Recent studies have shown that the current detector could operate efficiently up to a luminosity of $L_{ist} = 2 \times 10^{35}\ cm^{-2}s^{-1}$, but safety margins are not so large. It is precisely in this context that different upgrade projects have been proposed, which intend to strengthen new detectors, for the purposes of make them more resistant even in harsher working conditions, while the luminosity will be gradualy increased.

This thesis focuses especially on the VerTeX Detector (VTX) proposal (the one chosen for the final upgrade), whose program provides for replacing the whole VXD with fully-pixelated five layers at different distance from the beam pipe, equipped with the same tipe of sensor technology, which is the CMOS Depleted Monolihic Active Pixel Sensors (DMAPS).

The good results achieved by the ALICE experiment (LHC), which employed the same technology, have pushed for this solution which has proven to

be reliable and promising in maintaining low occupancy in substantial level of backgrounds and good radiation hardness even after irradiation.

In order to fullfil the physics requirements of Belle II experiments, a new silicon sensor is being designed, called OBELIX, exploiting the 180 nm TowerJazz Semiconductor process. Developments will ensure a faster, lighter and highly granular chip, reducing the material budget and as consequence improving tracks and vertices reconstruction despite the worse expected background environment.

OBELIX planning is based on studies done on previous prototypes, among which TJ-Monopix 2, whose characterization is the main topic of this work. Continuous laboratory measurements and beam test have conducted and are still in progress, in order to study the response of the matrix before and after irradiation, its power consumption and also to fully characterize its electrical features. In particular, the analysis presented in this thesis, has completely characterized the response of the pixel matrix, returning important results that have allowed to interpret data obtained from tests during the Test Beam at Desy in July 2022 and that are being used in the design of the OBELIX chip.

In chapter 1

1. Belle II and SuperKEKB (SKB) accelerator

The first chapter introduces some of the main unexplained aspects of the Standard Model (SM), on which the Belle II physics program is founded. A short description of the SuperKEKB accelerator and the Belle II detector's structure is also presented and in conclusion some highlights on the current state of measurements.

1.1 Physics program of the B-factories

The SM is a physics theory that describes three of the fundamental forces involving elementary particles, which are strong, weak and electromagnetic interaction (with the exclusion of the gravitational one). It classifies all the elementary constituents of matter in 4 main groups: quark, leptons, bosons and Higgs, as shown in Figure 1.1.

Figure 1.1: Particle classification in the Standard Model.

1.1.1 Open questions in SM

Despite the undeniable success of the SM in making predictions on physical phenomena, which have been experimentally verified with high precision over the years, there are many aspects of the Nature on which it is unable to give answers [?]. Some of them are listed in the following.

- Three generations of quark and leptons have been discovered, but it is not known wheter they should be the only ones and the reasons behind their mass hierarchy.
- Higgs mechanism is able to explain the cause of elementary particles' masses through spontaneous electro-weak symmetry breaking, but it is not clear wheter neutrinos could gain their masses through the interaction with the Higgs boson.
- Another open question is the matter-antimatter asymmetry in the Universe. Even though Charge-Parity (CP) violation is necessary to explain its current state, the observed quantity is several orders of magnitude less than needed to explain the matter domination over antimatter, which allowed the evolution of the universe as we know it today.
- In the SM the Cabibbo-Kobayashi-Maskawa (CKM) matrix describes the flavour-changing weak interaction through the mismatch between the quantum state of the freely propagating quarks. It could be parametrized by three mixing angles and a complex phase that is at the foundation of CP violation in the quark flavor sector. The fact that its elements are almost diagonal might suggest the existance of a new symmetry, that is unbroken at high energy (greater than the order of TeV).
- Several astrophysical observations have been postulated the existance of dark matter, but its origin and nature have not been explained yet.

All these topics encourage the research of new particles and processes that could give reasonable answers.
At the energy frontier, experiments like the Large Hadron Collider (LHC) in Geneve are looking for new particles created from the proton-proton collision with a center mass energy up to 14 TeV.
At luminosity frontier instead, the hint of new particles and mechanisms is searched in precision measurements of suppressed reactions in flavour physics or in the deviations from SM. The discrepancies indeed, could be interpreted as a clue of new physics beyond SM. The last is the Belle II approach.

In particular the experiment investigates the CP violation in the B mesons system and it also searches for new physics evidences in the decays of B and D mesons, in τ leptons and in the dark matter sector (DM).

1.1.2 Peculiarity of asymmetric B factories

The center of mass energy of Belle II experiment has its peak at the $\Upsilon(4S)$ resonance, such as $\sqrt{s} = 10.58$ GeV, which decays almost instantaneously into two B mesons (B^0 - $\bar{B}^0$) in nearly 96% of all cases.

The main task of the VerteX Detector (VXD) is to reconstruct the production and decay vertices of the particles originated from the beam collisions. This aspect is crucial to perform time-dependent measurements, core of the Belle II physics program.

The choice of the asymmetric configuration of the beams relies precisely in the requirement to boost the mesons in order to measure their life-time, exploiting the information on the distance between their decay vertices. In fact in a beam symmetric situation, they would have been produced at rest, decaying roughly at the same point or in any case at undetectable distances. The investigation of CP violating processes instead, requires to measure the decay time difference of the two B mesons and its uncertainty is dominated by that of the decay vertex measurement (order of hundreds microns). Let us look at this in more details.

SuperKEKB collides an electrons beam of 7 GeV (High Energy Ring, HER) with a positrons beam of 4 GeV (Low Energy Ring, LER) and for this configuration results a Lorentz boost factor of the $\Upsilon(4S)$ of $(\beta\gamma)_{\Upsilon(4S)} \approx 0.28$.

The same boost is also acquired by B mesons, because they are produced almost at rest ($m_{\Upsilon(4S)}$ - $m_{2B_0} \approx 19$ MeV). Moreover knowing that $\tau_B \simeq 1.5 \times 10^{-12}$ s and so $c\tau_B \simeq 450$ μm, we can compute the average flight distance travelled before decaying:

$$l = (\beta\gamma)_{\Upsilon(4S)} c\tau_B \approx 126\mu m \tag{1.1}$$

This value must be within the vertex detector sensitivity in order to distinguish the vertex decay and as consequence to make precision measurements of lifetimes, mixing parameters and CP violation. The six-layer VXD could determines the position of the vertices with a precision better than 100 μm, allowing to reconstruct secondary vertices, i.e. the decay position of the particles coming from B decays, and also from τ leptons and D mesons.

We want to take a closer look at the event kinematics (e.g. Figure 1.2). The two B mesons are produced in an entangled quantum state, so from the decay products of the first it is possible to assign its flavor (for example B^0, identifyed as B^0_{tag}) and accordingly that of the second, which will be the opposite ($\bar{B}^0$, called $\bar{B}^0_{phys}$).

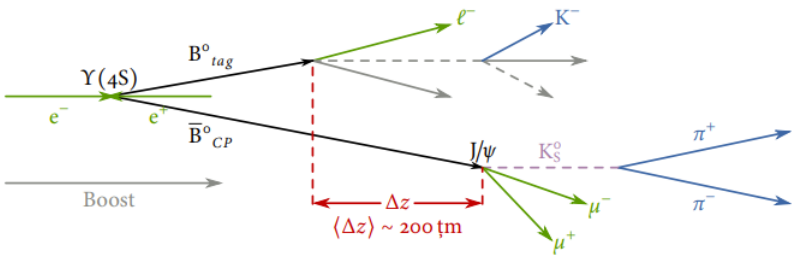

Figure 1.2: Example of the kinematics of the golden channel of Belle II experiment.

After this reconstruction, both B decay vertex positions in the longitudinal direction z_1 and z_2 are evaluated, in order to compute their difference:

$$\Delta z = z_1 - z_2 = (\beta\gamma)_{\Upsilon(4S)} c\Delta t \tag{1.2}$$

where Δt is the proper time decay difference. Another important parameter used in the reconstruction is d_0, which is the B decay vertex position from the primary vertex in the transverse plane.
Therefore this topology allows to transform a temporal information in a spatial one that we are able to measure. Without the boosted center of mass none of it could be possible, and this is an essential feature for an asymmetric B-factory.

1.2 SuperKEKB accelerator

Belle II sensitivity in the precision measurements is feasible expecially thanks to the extraordinary performance of the SuperKEKB accelerator which host the (almost) hermetic detector. This complex facility is the result of efforts and efficient collaboration between the researches of KEK laboratory and all the international working groups that partecipate to the experiment.

1.2.1 The facility

SuperKEKB (Figure 1.3) is an asymmetric e^+e^- collider with a circumference of 3 km and a center of mass energy peak equal to $\sqrt{s} = 10.58$ GeV, which corresponds to the mass of the $\Upsilon(4S)$ resonance. Compared to its predecessor KEKB (which started its operation in 1998 and concluded it in 2010), the current accelerator has allowed to obtain the highest luminosity ever achieved, equal to $4.7 \times 10^{34}\ cm^{-2}s^{-1}$ in July 2022. This target was possible using a new scheme to accelerate and collide the beams, the so called *nano-beam scheme* (subsection 1.2.2).

Furthermore a new upgrade of the machine, still under study, will also include other interventions expecially to cope with higher background levels, in view of a future increase in luminosity.

Luminosity

Istantaneous luminosity is one of the key parameters of any accelerator and it represents the interaction rate per unit of cross section between colliding particles. Reversing this equation is possible to obtain N, namely the number of the physical events produced in the interaction with a given luminosity:

$$L = \frac{1}{\sigma}\frac{dN}{dt} \qquad \Rightarrow \qquad N = \int_0^T L\sigma dt \tag{1.3}$$

where T is the duration of the experiment, σ the cross section of the physical process of interest. Although this is a raw information, as it does not consider other important factors that could influence the effective number of events produced, it becomes a significant starting point when one wants to study very rare processes such as Belle II. Specifically luminosity is strictly dependent from both machine and beam parameters. With respect to this, it can be expressed as:

$$L = \frac{\gamma_\pm}{2er_e}\left(1 + \frac{\sigma_y^*}{\sigma_x^*}\right)\left(\frac{I_\pm \xi_{y\pm}}{\beta_y^*}\right)\left(\frac{R_L}{R_{\xi_{y\pm}}}\right) \tag{1.4}$$

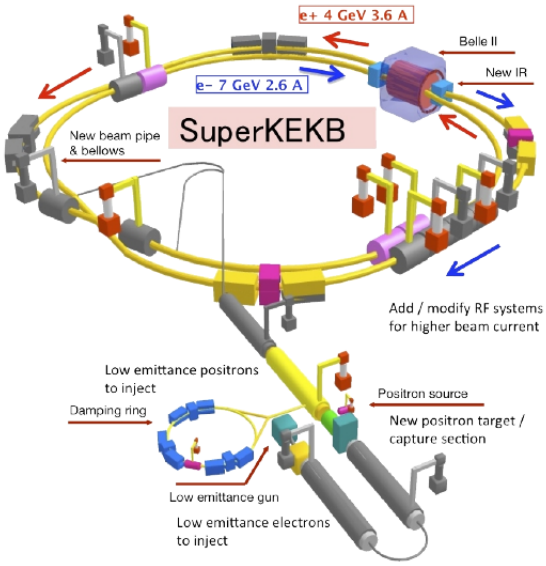

Figure 1.3: SuperKEKB accelerator structure.

where "±" denotes respectively positrons and electrons beam, $\sigma^*_{x,y}$ is the beam size at the Interaction Point (IP) in the horizontal and vertical plane, I is the beam current, β^*_y the vertical beta function at the IP. $\xi_{y\pm}$ is the vertical beam parameter which include the horizontal beta function at the IP, the horizontal emittance, the bunch lenght and the crossing angle between the beams. R_L and $R_{\xi_{y\pm}}$ are the reduction factors due to geometrical loss such as the hourglass effect and finite crossing.

As already mentioned, SuperKEKB holds the actual world record in luminosity (with β^*_y= 1.0 mm) and in the near future the target will be to reach $6 \times 10^{35}\ cm^{-2}s^{-1}$ (by the 2030s), by increasing current beams and reducing their section at the IP, through the decrease of the betatron function down to $\beta^*_y = 0.3$ mm. But this process makes the beam-induced background grow a lot, risking deterioration and poor functioning of the detectors.

For these reasons the supervision of the beams background becomes crucial: right now it has been estimated that the background should remain accettable up to a luminosity value equal to $2.8 \times 10^{35}\ cm^{-2}s^{-1}$ with β^*_y= 0.6 mm. So the chance to achieve higher luminosity is closely related to an upgrade plan of both the whole detector and the accelerator.

1.2.2 "Nano-beam" scheme

We have seen that the *beta function* β at the IP (β^*) is a decisive factor to define the luminosity. To be able to ramp the luminosity up, it is necessary to reduce the value of β depending also, but not only, on the variation of the other machine parameters that appear in the Equation 1.4.

The mechanism used in SuperKEKB is called *nano-beam scheme*, and it allowed to obtain luminosity 40 times greater than that of KEKB, managing to

decrease of 1/20 the β^*.

This new scheme, originally designed by P. Raimondi, dictates that the beam bunches have to collide with sufficiently small σ_x^* and at large angle. In case of SuperKEKB the latter is equal to 83 mrad at the IP (larger with respect to the crossing angle used in KEKB) with the beam size of 50 nm in the vertical direction and 100 μm in the horizontal direction (in Figure 1.4 a simplified representation of the differences).

This strategy also helps to reduce the *hourglass effect*, which happens when the β^* is comparable or smaller than the bunch lenght, causing a decrease in luminosity. As a matter of fact with larger crossing angle at the IP, the overlap lenght which is the effective bunch lenght, is much shorter than the bunch length along the beam axis.

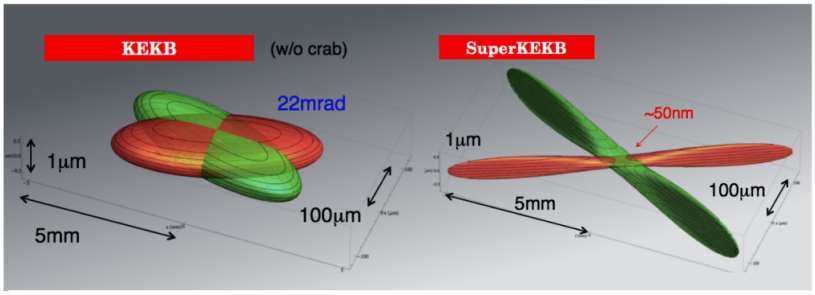

Figure 1.4: Comparison between the beam schemes used in KEKB and SuperKEKB.

Using a crossing angle large enough has other positive implications on the operation of the accelerator and its further improvements, like allowing the placement of a new focusing system at the IP (which may require more space), considering a future redesign of the interaction region.

1.3 Belle II detector

The Belle II detector is a general-purpose spectrometer which consists of a nested subdetectors sequence placed around the berillium beam pipe of 10 mm radius, nearby the IP of the two beams. Here we will go trough a briefly description of the several subdetectors (Figure 1.5) going in order from the beam pipe outwards: the Vertex Detectors, the Central Drift Chamber, the TOP and the ARICH, the electromagnetic calorimeter and the K_L muon detector.

1.3.1 Vertex Detectors (VXD)

The **VerteX Detector (VXD)** is composed by two devices divided into layers, the silicon Pixel Detector (PXD) and the Silicon Vertex Detector (SVD), for a total of six layers around the beam pipe.
The inner two layers of PXD (L12) consist of pixelated sensors based on the depleted field effect transistor (DEPFET) techonology, realised with very thin (<

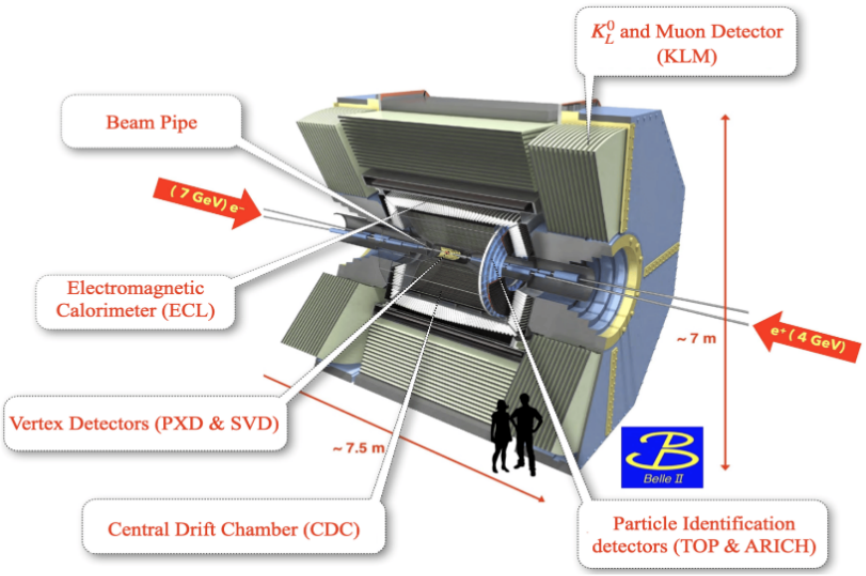

Figure 1.5: Belle II detector.

100 μm) sensors which allows to minimise multiple scattering, thus improving the tracking resolution for low-momentum particles. They are at a radius of 14 mm and 22 mm, respectively.
The remaining four layers of SVD (L3456) instead, are equipped with double-sided silicon strip (DSSD) sensors (at 39 mm, 80 mm, 104 mm and 135 mm respectively). Since a lower background rate is expected with respect to PXD, DSSD allow to achieve similar performance with a much smaller number of readout channels. These layers are mainly used for tracking/vertexing and also for particle identification (PID), through the measurement of the energy loss (dE/dx).

We can notice in Figure 1.6 that because of the essential asymmetric configuration of the beam energies and the consequent boost of the particles produced in the collisions (subsection 1.1.2), the structure of the vertex detectors is also asymmetric along the logitudinal axis.

1.3.2 Central Drift Chamber (CDC)

This is the central tracking device, with a large-volume drift chamber and small drift cells. The chamber gas is composed of a He$-$$C_2H_6$ (50:50) mixture with an average drift velocity of 3.3 cm μs^{-1} and a maximum drift time of about 350 ns for a 17 mm cell size.
The CDC contains 14336 wires arranged in 56 layers either in *axial* (aligned with the solenoidal magnetic field) or *stereo* (skewed with respect to the axial wires) orientation (Figure 1.7). In fact by combining information from both the axial and the stereo layers it is possible to reconstruct full three-dimensional helix charged tracks and measure their momenta. It also provides information for PID by measuring ionization energy loss, which is particularly useful for low-

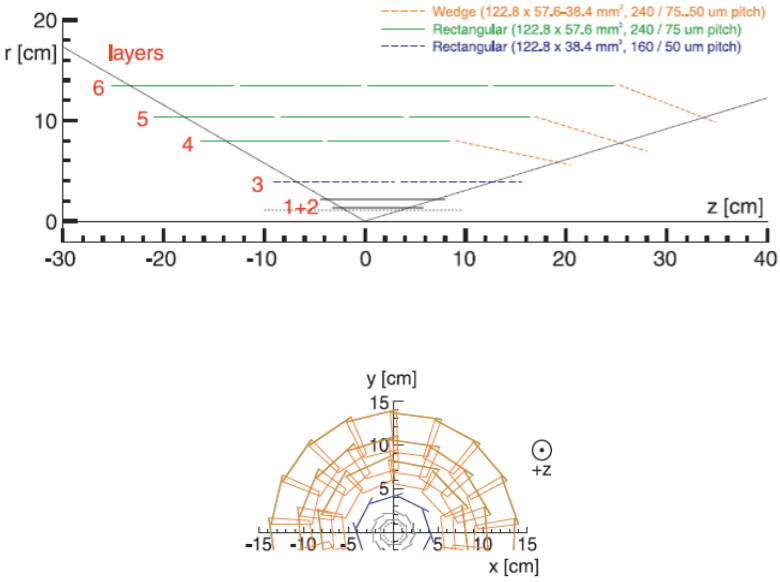

Figure 1.6: A schematic view of the Belle II vertex detector with a Be beam pipe and the six layers of PXD and SVD.

momentum particles that cannot reach the outer subdetectors dedicated also to deal with PID.

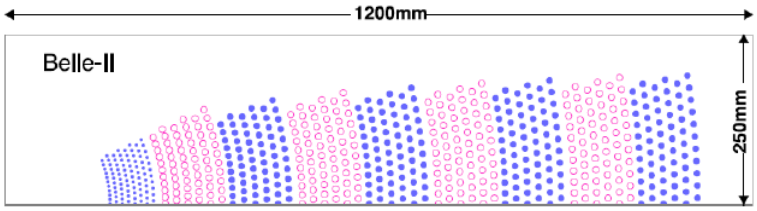

Figure 1.7: Schematic view of the CDC drift cells: blue dots represent the axial wires and the pink empty ones the stereo wires.

1.3.3 Particle identification system (TOP e ARICH)

TOP (Time Of Propagation) is a special kind of Cherenkov detector used for PID in the barrel region. It employs the two-dimensional information of a Cherenkov ring image, such as the time of arrival and the impact position of Cherenkov photons at the photodetector at one end of a 2.6 m quartz bar. It is composed by 16 detector modules, each one consisted in a 45×2 cm quartz bar (Cherenkov radiator) with a small expansion volume (about 10 cm long) at the sensor end of the bar (Figure 1.8).

In order to achieve a single-photon time resolution of about 100 ps (required for a good PID), 16-channel of microchannel plate photomultiplier tubes (MCP-

PMT) are employed, specially developed for this purpose.

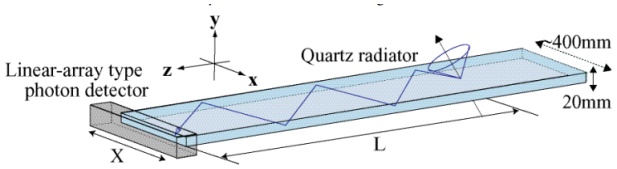

(a) A schematic view of the TOP radiator.

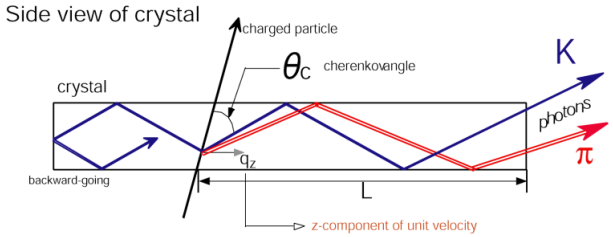

(b) A side view of the TOP radiator.

Figure 1.8: TOP detector.

ARICH (Aerogel Ring Imaging CHerenkov) is used to identify charged particles and it is placed in the forward endcap region. It is a proximity focusing Cherenkov ring-imaging detector which adopts aerogel as Cherenkov radiator. In particular this detector employs a novel method to increase the number of detected Cherenkov photons: two 2 cm-thock layers of aerogel with different refractive indices (n_1 = 1.045 upstream, n_2= 1.055 downstream) that increase the yield without degrading the Cherenkov angle resolution (Figure 1.9).

A hybrid avalanche photon detector (HAPD) are exploited as single-photon-sensitive high-granularity sensor. Here photo-electrons are accelerated over a potential difference of about 8 KV and are detected in avalanches photodiodes (APD).

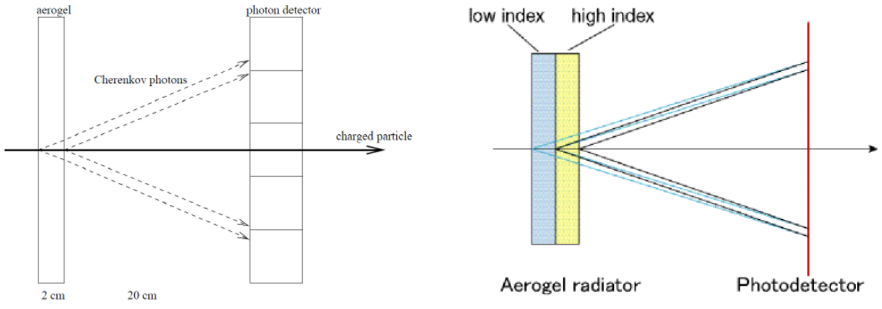

Figure 1.9: ARICH detector.

The main task of these detectors is to improve the K/π separation until 3.5 and 4 GeV/c of momentum, respectively.

1.3.4 Electromagnetic calorimeter (ECL)

The **ECL** is a highly segmented array of tallium-doped caesium iodide CsI(Tl) crystals assembled in a 3 m long barrel section with a radius of 1.25m, and two endcaps discs located at 2 m (forward) and 1 m (backward). All of them are instrumented with a total of 8736 crystal, covering about 90% of the solid angle in center-of-mass system.

This detector is used to detect gamma rays and to identify electrons in order to separate the latter from hadrons, expecially pions.

1.3.5 K_L muon detector (KLM)

It consists of an alternating sandwich of 4.7 cm-thick iron plates and active detector elements located outside the volume of the superconducting solenoid that provides a 1.5 T magnetic field. The iron plates serve as the magnetic flux return joke for the solenoid. They also provide 3.9 interaction lenghts or more of material, beyond the 0.8 interaction lenghts of the calorimeter in which K_L^0 mesons can shower hadronically. The active detector elements have been chosen in order to cope with the reduction of the detector efficiency under the SuperKEKB background rates: resistive plate chambers (RPCs) for the outermost active layers and in the two innermost layers of the barrel and endcaps regions, scintillator strips with wavelenght-shifting fibers are used, readout by silicon photomultipliers (SiPMs).

In Figure 1.10 a summary of the main characteristics of all subdetectors.

Purpose	Name	Component	Configuration	Readout channels	θ coverage
Beam pipe	Beryllium		Cylindrical, inner radius 10 mm, 10 μm Au, 0.6 mm Be, 1 mm paraffin, 0.4 mm Be		
Tracking	PXD	Silicon pixel (DEPFET)	Sensor size: 15 × (L1 136, L2 170) mm^2, pixel size: 50 × (L1a 50, L1b 60, L2a 75, L2b 85) μm^2; two layers at radii: 14, 22 mm	10 M	[17°; 150°]
	SVD	Silicon strip	Rectangular and trapezoidal, strip pitch: 50(p)/160(n)–75(p)/240(n) μm, with one floating intermediate strip; four layers at radii: 39, 80, 104, 135 mm	224 k	[17°; 150°]
	CDC	Drift chamber with He–C_2H_6 gas	14 336 wires in 56 layers, inner radius 160 mm, outer radius 1130 mm	14 k	[17°; 150°]
Particle ID	TOP	RICH with quartz radiator	16 segments in ϕ at $r \approx 120$ cm, 275 cm long, 2 cm-thick quartz bars with 4 × 4-channel MCP PMTs	8 k	[31°; 128°]
	ARICH	RICH with aerogel radiator	2 × 2 cm-thick focusing radiators with different n, HAPD photodetectors	78 k	[14°; 30°]
Calorimetry	ECL	CsI(Tl)	Barrel: $r = 125$–162 cm, endcap: $z = -102$–+196 cm	6624 (barrel), 1152 (FWD), 960 (BWD)	[12.4°; 31.4°], [32.2°; 128.7°], [130.7°; 155.1°]
Muon ID	KLM	barrel: RPCs and scintillator strips	2 layers with scintillator strips and 12 layers with 2 RPCs	θ 16 k, ϕ 16 k	[40°; 129°]
	KLM	endcap: scintillator strips	12 layers of (7–10)×40 mm^2 strips	17 k	[25°; 40°], [129°; 155°]

Figure 1.10: Summary of the main characteristics of all subdetectors.

1.3.6 Trigger system

The trigger system of Belle II has a non-trivial role to identify events of interest during data-taking at SuperKEKB, where high background rates are expected.

This system is divided into two levels: a hardware-based low-level trigger (L1) and a software-based high-level trigger (HLT), implemented in the data acquisition (DAQ) system.

- **L1**: has a latency of 5 μs and a maximum trigger output rate of 30 kHz, limited by the read-in rate of the DAQ.
- **HLT**: is a key component of the DAQ, used to fully reconstruct events that pass the L1 trigger selection. It has to reduce online event rates to 10 kHz for offline storage and it must identify track regions of interest for PXD readout in order to reduce data flux. It fully recreates events with offline reconstruction algorithms, using all detectors infromation except for the PXD.

1.4 Current state of data taking

SuperKEKB accelerator reaches a new luminosity peak of $4.7 \times 10^{34}\ cm^{-2}s^{-1}$ in July 2022 (Figure 1.11).

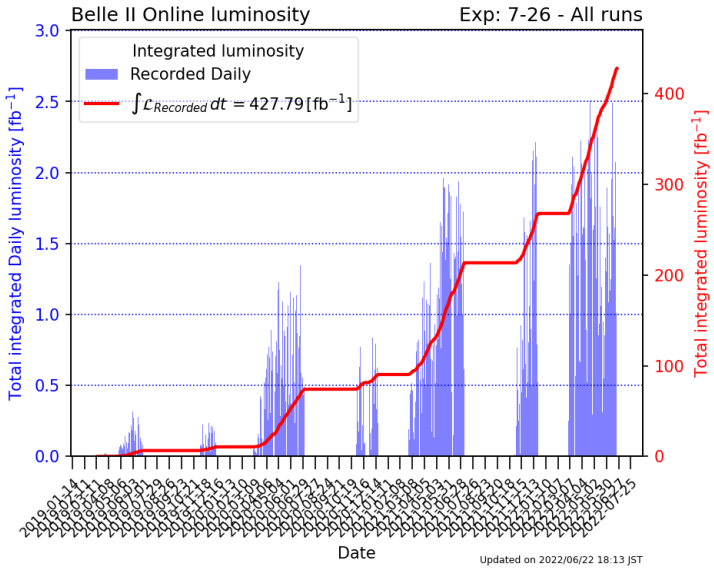

Figure 1.11: Total recorded integrated luminosity before Long Shutdown 1.

In further perspectives, the target of SuperKEKB is to achieve a new record with $L_{ist} = 6 \times 10^{35}\ cm^{-2}s^{-1}$ and to increase the integrated luminosity from 428 fb^{-1} (current value, starting in 2019) to 50 fb^{-1} (projection plot shown in Figure 1.12), in order to increase the statistics and as consequence the hope to give an insight in some of the questions still open in the SM.

To accomplish the fixed goals mentioned above, an upgrade not only of the vertex detector but also of the whole experiment and of the interaction region is necessary, among several reasons, to cope with a more complex circumstances due to the increased luminosity which undermine its proper functioning.

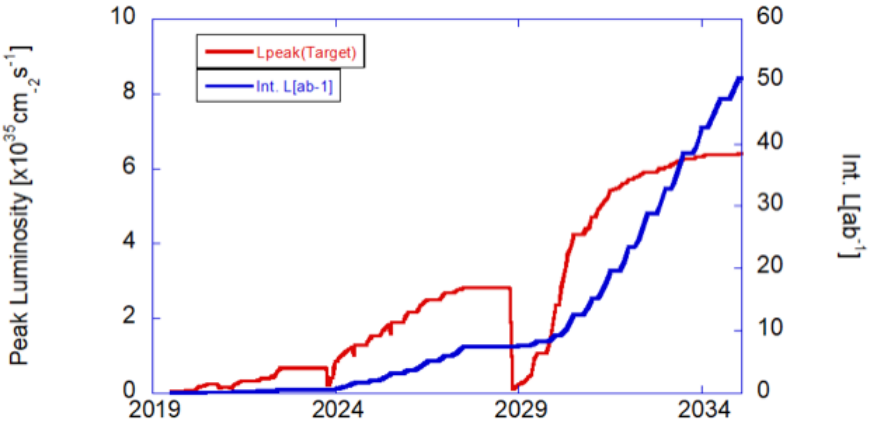

Figure 1.12: Luminosity projection plot (plan for the coming years).

Therefore a three-phase program has been drawn up:

- **short term**: year 2022. Long Shutdown 1 (LS1) is planned for approximately 15 months starting in July 2022, in order to install a complete pixel detector (PXD).
- **medium term**: approximately year 2028-29. Long Shutdown 2 (LS2) will probably be needed for the upgrade of the Interaction Region (IR) to reach a new luminosity target $L_{peak} = 6 \times 10^{35}\ cm^{-2}s^{-1}$. Several open questions and difficulties have triggered many studies and discussions about a possible redesign of the machine lattice during this phase. In particular it would be necessary to deal with the limitation of the optics of the machine, concerning the further increasing of the luminosity and accordingly of the backgrounds rates. A new Vertex Detector might be also required, to accommodate the new IR design, and other sub-detector upgrades are possible.
- **long term**: years $>$ 2032. Studies have started to explore upgrades beyond the currently planned program, such as beam polarization and ultra-high luminosity and so possibly L_{peak} in excess of $1 \times 10^{36}\ cm^{-2}s^{-1}$. While the beam polarization has a concrete proposal, for ultra-high luminosity studies have just started.

At time of writing we are in the period of a long shut-down (LS1), last since June 2022 and the installation of a complete pixel detector (PXD) is almost done. The restart of data taking is planned at the beginning of 2024.

2. CMOS MAPS sensors

The fourth chapter aims to introduce the essential features of the semiconductor detector technology, going through the history of its advancements, which have led to the currently most promising sensors based on CMOS logic structure, the Monolithic Active Pixel Sensors (MAPS). As we have seen in the previous chapter, the VTX program wants to make the most of the technologies that have already proven reliable in precision measurements, like the TJ-Monopix development line. We will briefly present it, mentioning the peculiarities of its prototypes, to better understand how they could fulfill the Belle II requirements.

2.1 Semiconductor detectors

2.2 Hybrid and monolithic pixel sensors

2.3 CMOS Monolithic Active Pixel Sensors technology

2.4 History of Monopix developments

3. Conclusions

List of Figures

1.1 Particle classification in the Standard Model. 6
1.2 Example of the kinematics of the golden channel of Belle II experiment. 8
1.3 SuperKEKB accelerator structure. 10
1.4 Comparison between the beam schemes used in KEKB and SuperKEKB. 11
1.5 Belle II detector. 12
1.6 A schematic view of the Belle II vertex detector with a Be beam pipe and the six layers of PXD and SVD. 13
1.7 Schematic view of the CDC drift cells: blue dots represent the axial wires and the pink empty ones the stereo wires. 13
1.8 TOP detector. 14
1.9 ARICH detector. 14
1.10 Summary of the main characteristics of all subdetectors. 15
1.11 Total recorded integrated luminosity before Long Shutdown 1. . . 16
1.12 Luminosity projection plot (plan for the coming years). 17

List of Tables